International Core Journal of Engineering Volume 5 Issue 10, 2019
ISSN: 2414-1895 DOI: 10.6919/ICJE.201909_5(10).0044

Robust Load Frequency Control on Ship Integrated Power System Using H∞ and μ-Synthesis Approaches

Jian Chen, Dan Yu, Xihuai Wang, Hongyue Li

Logistics Engineering College of Shanghai Maritime University, Shanghai, China

Abstract

This paper focuses on Load Frequency Control (LFC) on ship Integrated Power System (IPS). In the ship IPS with energy storage, the load frequency is fluctuated significantly by external disturbance such as the load change and internal parameters perturbation such as battery internal resistance, damping or inertia coefficient of power system, and hence design a controller to keep the frequency stable is necessary. In response to these problems, the H∞ and μ-synthesis robust control approaches respectively based on mixed sensitivity principle and structure singular value are used to deal with the load frequency control. In the proposed control scheme, the batteries are utilized to balance the load power and diesel generators output power and the state space model of two-area interconnected power system on the ship is established. The controllers' robust stability and robust performance based on H∞ and μ-synthesis are verified in the presence of external disturbances and parametric perturbation. The results are simulated in computer and compared with classical PI controller. It is show that both the H∞ and μ-synthesis controllers have good performances than classical PI controller and the μ-synthesis controller provides better performance than the H∞ control method due to considering parameter perturbation.

Keywords

Load frequency control; Ship integrated power system; H∞ control; μ-synthesis analysis; Robust control; Uncertainty.

1. Introduction

With the development of power electric technology, relevant experts devote themselves to study on the application of renewable energy on the ship integrated power system (IPS), such as wind, solar[1-5], and the new structure of ships make them more and more like the land micro-grid. However, because of the instability and randomness of renewable energy, it is hard to keep the frequency stable on the IPS. Due to the controllability of the energy storage unit (battery, super capacitor, flywheel), it is researched and applied by relevant experts in order to keep the power balance and improve the load transient response, also enhance the fuel economy of the diesel generators[6-10].

The ships are working as an isolated system, have strict requirements of stability and reliability. Due to the weather reasons and the working environment, the hybrid electric ships have more frequently power disturbance and large scale perturbation of system parameters, these reasons can lead the system power unbalance, and bring the frequency fluctuation. Although the control methods for land grid can be referenced to use to the ship power systems, but because of the special characteristic, the methods cannot work well for ships. Traditionally, droop control and frequency and load modulating control are utilized to keep the frequency stable. For a small frequency deviation, the droop control can suppress fluctuation quickly, but the droop control cannot bring the frequency to the reference value if the deviation is big. Frequency and load modulating control can eliminate the big deviation

ISSN: 2414-1895 DOI: 10.6919/ICJE.201909_5(10).0044

through change the governor characteristic and bring the deviation to zero, but this process is longer than droop control. For the land grid, the load frequency control (LFC) is researched widely to keep the power system frequency stable, and many of control methods are researched to design the load frequency controllers.

The PI or PID controllers, because of their simple structure and can be designed easily, have been used widely in the power system to control the load frequency. In order to find the optimal value of the controller coefficients, the integral of time multiplied absolute error (ITAE) or integral of square error (ISE) are defined to a performance index and as the constraint conditions, differential evolution algorithm[11,12], fuzzy logic algorithm[13]，or particle swarm optimization (PSO)[14] algorithm are utilized to solve the multi objective constraint problem. Compared with the conventional controller, the optimized controllers have much better dynamic performance. In [15,16], a kind of fractional order PID (FOPID) has been designed to eliminating the frequency deviation. In [17], a PID controller optimized by chaotic algorithm is proposed to control the interconnection power system. The simulation results showed that the optimized PID controllers have able to keep the load frequency stable in power system and have a better control performance, but the robustness and robust stability of the controllers are not satisfied.

With the development of the control theory, some intelligent algorithms also have been applied to design the LFC controller. In [18-21], the model predictive control is considered to solve the frequency unstable problem in an interconnection power system with multivariable uncertainty. In [22], the fuzzy logic method is designed as the LFC controller in the micro-grid. The fuzzy logic control has a good robust stability and robust performance because this method use uncertain language to describe the certain system, for thus, the uncertain disturbance of the system can be controlled well by the method, but the control accuracy cannot guaranteed by this method. In [23-25], aiming at the isolated micro-grid system with solar and diesel generator, a sliding mode control based on load estimation is proposed. Through the estimation of the disturbance power and the frequency deviation, the sliding mode compensation controller is designed to control the active power outputted from the diesel generator set. This method has good robustness and reduces the controller design cost.

All the methods mentioned above have better performance for the frequency control of the micro-grid system, and the designed controllers have better robustness and satisfactory control precision. However, the load frequency control with uncertain disturbance is a complicated nonlinear system, for the land grid, it can be seen as infinite system, the approximate linearization in the modeling process does not affect the overall performance of the system. But for the ship power system, the load motor and the generator usually have the same capacity, the motors start or stop and variable load operation will bring a huge impact to the ship power grid, meanwhile, affected by wind or waves, the generation side output power and the demand power cannot maintain balance. Although the above control strategies of the land grid can be considered to design the secondary frequency controller for the ship micro-grid, it is difficult to ensure the robustness and control precision of the controller.

Considering the frequency deviation is usually caused by power disturbance and parameter perturbation, in [26], the H∞ load frequency controller is designed to deal with the external disturbance, but the parameter perturbations are not studied. The H∞ method always brings the conservation to deal with the parameter perturbation problem, for this, μ-synthesis method is the better choice. In[27]，the μ-synthesis method is utilized to designed the LFC controller, but the comparison between H∞ and μ-synthesis is not given. In this paper, the H∞ and μ-synthesis robust control is studied to design the load frequency controller of ship power system, both the control effects are given.

Following the introduction in Section I, the rest of the paper is organized as follows. In Section II, the HIPS structure is described and the state space modeling of LFC is established. H∞ and μ-synthesis theory is presented briefly in Section III. The controllers designed via H∞ and μ-synthesis is presented in Section IV and V respectively. In Section VI, the result is simulated and verified. Finally, the conclusion is presented in Section VII.

ISSN: 2414-1895 DOI: 10.6919/ICJE.201909_5(10).0044

2. Hips Modeling

In this section, the ship integrated power system model is described, then the state space equation of LFC is established, and the uncertainties in the system are explained.

2.1 IPS Model on Ship

The new type ship integrated power system researched in this paper is composed of conventional diesel generators and battery, the structure is described in Fig.1.

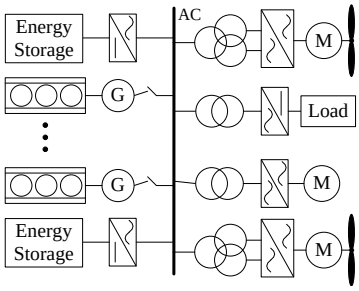

Fig.1 Simplified model of HIPS

The diesel generators, as the most important part of the ship, undertake the mostly output power to the system, and the generator rotor speed determinate the power frequency stable or not. When a big disturbance occurred, such as the propellers turn on or turn off, it will take a long time for the governor to stable the frequency. Considered the battery has the ability to absorb or release energy from the system, it can be used in the ship power system to improve the system stability. In order to enhance the fault tolerance and satisfied the high power requirement, two or more diesel generators are needed and divide them in two areas. The output power and demand power of the system are satisfied as:

$$\Delta P_{deg} + \Delta P_{bat} = \Delta P_{load} + \Delta P_{dem} \tag{1}$$

Where, $\Delta P_{\deg}$ is the diesel generator output power deviation, ΔP_{bat} is battery output power deviation, ΔP_{load} is load disturbance power deviation, and ΔP_{dem} is the demand power deviation. The system load frequency will be unstable if the equation (1) is not match between the right side and the left side.

2.2 State Space Dynamic Model

In this paper, four diesel generators are needed to meet the high power demand of the ship, and each area include two diesel generators and one battery. The diesel generators and batteries have the same parameters and the same capacities. The secondary frequency control of ship power system is shown in Fig.2. The control objective is to ensure that the load frequency deviation of each sub-area can return back to zero when the system is disturbed. Meanwhile, the tie-line power between two interconnected areas also be bought to zero whichever area is disturbed.

In the figure, β_i is scale factor, K_i is gain factor, R_i is droop constant, T_{gi} is governor time constant, T_{di} is diesel time constant, T_{bi} is battery time constant, M_i is inertia coefficient, D_i is damping coefficient, Δf_i is frequency deviation, Δu_i is system input deviation, T_{12} is synchronization time constant, ΔX_i is governor output deviation, ΔP_{gi} is diesel generator output power deviation, ΔP_{bi} is battery output power deviation, ΔP_{Li} is load power deviation, ΔP_{tie} is tie-line power deviation, and $i = 1,2,3,4$ .From the figure, the load frequency control state space model can be established:

$$\begin{aligned} \dot{x} &= Ax + Bu + \Gamma w \\ y &= Cx \end{aligned} \tag{2}$$

$x = [\Delta P_{g1}; \Delta P_{d1}; \Delta P_{b1}; \Delta f_1; \Delta P_{tie}; \Delta P_{g2}; \Delta P_{d2}; \Delta P_{b2}; \Delta f_2]$ is the state variable of system, u is the control input, y is the system output, w is the disturbance input. The matrices are shown in the Appendix.

The diesel generators and batteries capacity are listed in Tab.1.

ISSN: 2414-1895 DOI: 10.6919/ICJE.201909_5(10).0044

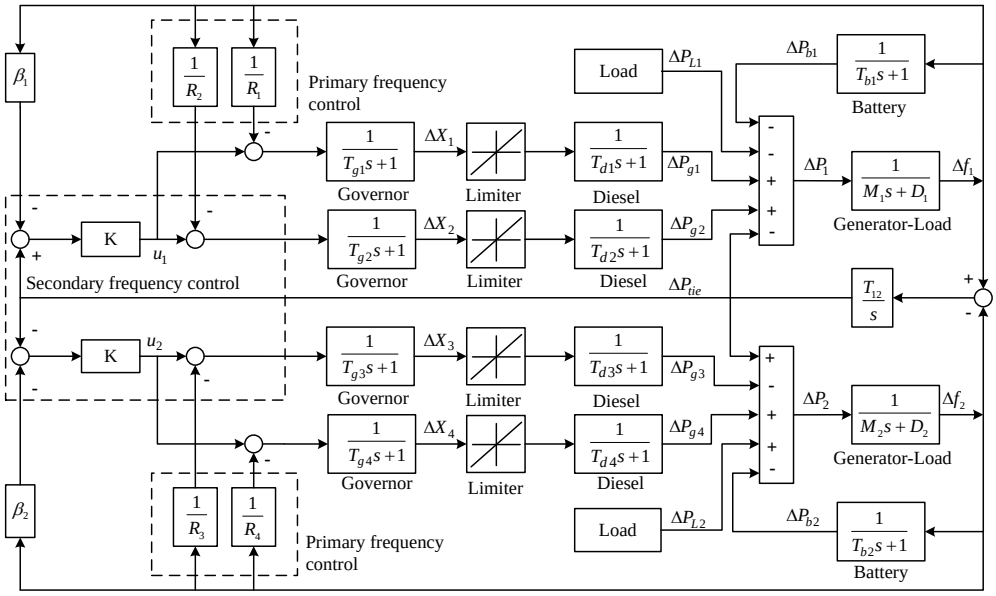

Fig.2 Load frequency control of two area ship power system

Tab.1 System parameter

Parameter	Value
Rated Frequency [Hz]	50
Diesel Generator Capacity [MW]	1.5
Battery Capacity [KWh]	1.0
Propulsion Motor Capacity [MW]	2.2
Governor Time Constant T_g [s]	0.08
Diesel Time Constant T_d [s]	0.3
Battery Time Constant T_b [s]	0.01
Inertia coefficient M	12.5
Damping coefficient D	0.8
Droop coefficient R	2.4
Ratio coefficient β	-1

2.3 Uncertainty Model

The mathematical expression (2) described the load frequency control on SIPS, Δf is considered as the output signal and the aim of the control is minimizing Δf regardless how the perturbation vary. However, a physical system is disturbed by external disturbance and the system inner parameters are not stable at all times, so the actual system cannot be described exactly by mathematical model. The model uncertainty can be expressed as:

$$P_A(s) = P(s) + \Delta(s) \tag{3}$$

Where, $P_A(s)$ is the actual controlled plant, $P(s)$ is the nominal model and $\Delta(s)$ is the system errors, which is a Block Diagonal Bounded Perturbation(BDBP). Two types of uncertainty defined in the following should be taken into consideration while designed a good controller:

ISSN: 2414-1895 DOI: 10.6919/ICJE.201909_5(10).0044

1) Structured uncertainty: can be considered as the parameters perturbation due to the aging of the device or measurement error.

2) Unstructured Uncertainty: can be considered as the external or neglected dynamics of the plant.

3. H∞ AND μ-SYNTHESIS

H∞ and μ-synthesis theory is briefly introduced in this section

3.1 H∞ Control Based on Mixing Sensitivity

Considering the feedback control system shown in Fig.3, for the disturbance signal w, the sensitivity function $S(s)$ and the complementary sensitivity function $T(s)$ can expressed as:

$$S(s) = [I + P(s)K(s)]^{-1}$$
$$T(s) = [I + P(s)K(s)]^{-1}P(s)K(s) \tag{4}$$

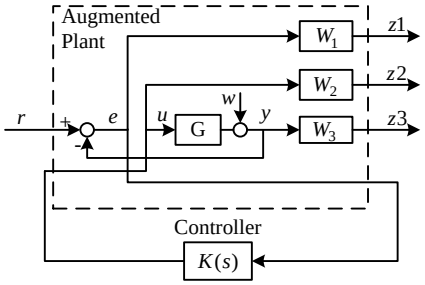

Fig.3 Mixed sensitivity control

In order to suppress the affect from the disturbance signal w to the output signal y, the sensitivity function $S(s)$ is required the smaller the better, and this is the so-called minimum sensitivity control problem, i.e. finding a controller K to stable the system P and guarantee $S(s)$ minimum. According to the $H\infty$ norm definition, the minimum sensitivity control problem can be translated into a $H\infty$ control problem: $\min\|S(s)\|_\infty$.

In order to guarantee the robust stability of control plant with model uncertainty, the complementary sensitivity function $T(s)$ is also required the smaller the better, so this is contradict with the sensitivity function $S(s)$, and a compromise treatment is considered between $S(s)$ and $T(s)$ and can be expressed as:

$$\left.\begin{aligned}\|S(j\omega)\|_\infty < \varepsilon_1, \omega \in \Omega_1 \\ \|T(j\omega)\|_\infty < \varepsilon_2, \omega \in \Omega_2\end{aligned}\right\} \tag{5}$$

Where, $\varepsilon_1, \varepsilon_2$ are positive and Ω_1, Ω_2 are frequency domain with no common part. As usual, the perturbation signal behaves as a low frequency characteristic while the model uncertainty presents a high frequency characteristic, based this, Ω_1 is low frequency domain and Ω_2 is high frequency domain generally. Because the controller presented in formula (5) is difficult to figure out, so the controller can further be presented as:

$$\left\|\begin{bmatrix} W_1 S \\ W_2 T \end{bmatrix}\right\|_\infty < \gamma \tag{6}$$

Where, W_1 and W_2 are weighted functions with larger values in Ω_1 and Ω_2 respectively, γ is positive, without loss of generality, it can be valued as 1. This is the mixed sensitivity control problem.

3.2 μ-Synthesis and Analysis

In a practical control problem, the different or error are ineluctable between the mathematical model and the actual model of the researched system. These errors must be considered when the controller is designed to guarantee the robust stability and robust performance of system. However, the H∞

ISSN: 2414-1895 DOI: 10.6919/ICJE.201909_5(10).0044

approach may achieve robust stability and the robust performance is less than satisfactory. The μ-synthesis based on structured singular value can solve this problem and reduce the robust design conservative because the robust stability and robust performance are considered when the controller is designing.

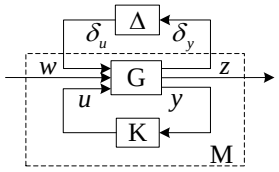

Fig.4 General control system

For a system $\boldsymbol{M}$ shown in Fig.4, the uncertainty can be modeled as norm bounded uncertain block with diagonal structure $\boldsymbol{\Delta}$, the structured singular value μ defined as:

$$\mu_{\Delta}(\boldsymbol{M}) = \frac{1}{\inf\limits_{\Delta\in\underline{\Delta}}\{\sigma_{\max}(\Delta) : \det(\boldsymbol{I} - \boldsymbol{M}\Delta) = 0\}} \tag{7}$$

From the expression, we can see that the inverse of the maximum singular value reflect the minimum margin of unstructured uncertainty $\boldsymbol{\Delta}$ what can caused the feedback system unstable. In other words, the peak value determines the uncertainty of feedback control system robust stability. For the system consist of nominal model and uncertain weighting function, via linear fractional transformation $\boldsymbol{M} = F_l(\boldsymbol{G}, K)$, the robust stability and robust performance evaluation index can be obtained. Assumed that $\gamma > 0$, for each $\Delta(s) \in \underline{M}(\Delta)$ which satisfied $\|\Delta\|_\infty < \gamma^{-1}$, the sufficient and necessary conditions for the feedback control system shown in Fig.4 to be stable is $\sup\limits_{\omega\in R}\mu_{\Delta}(G(j\omega)) \le \gamma$. This pointed out the robust stability condition for the system. Meanwhile, the robust performance condition for the system is that: Assumed that $\gamma > 0$, for each $\Delta(s) \in \underline{M}(\Delta)$ which satisfied $\|\Delta\|_\infty < \gamma^{-1}$, the sufficient and necessary condition for the feedback control system to be stable and well-posed, and satisfied $\|F_l(G_p, \Delta)\|_\infty \le \gamma$ is $\sup\limits_{\omega\in R}\mu_{\Delta_p}(G_p(j\omega)) \le \gamma$.

3.3 DK Iteration

DK iterative is a common method to solve the μ-synthesis controller. The steps are following:

Step 1: Select the initial scale matrix D, set $D = I$ generally;

Step 2: Hold D, minimize K and obtain the optimum solution via H∞ optimization method;

Step 3: Hold K to solve the convex optimization problem for D and obtain the optimal estimation matrix mark as $\tilde{D}$.

Step 4: Compared D and $\tilde{D}$, if the two is closer, the controller K is the optimal controller, otherwise, let $D = \tilde{D}$ and return to step 2.

Through the DK iterative process, the controller is solved.

4. Controller Designed Based on H∞

In this section, the H∞ controller is designed based on Linear Matrix Inequality (LMI). And the amplitude frequency characteristic and robust performance is verified respectively.

The H∞ controller based on mixed sensitivity for the LFC on HIPS is solved by LMI. The designed controller satisfies:

$$\left\| \begin{matrix} (I+GK)^{-1} \\ K(I+GK)^{-1} \end{matrix} \right\|_\infty < \gamma \tag{8}$$

Where, $\gamma > \gamma_0 := \min\limits_{Kstabiling} \|F_L(G,K)\|_\infty$, and the controller can be solved as following:

ISSN: 2414-1895 DOI: 10.6919/ICJE.201909_5(10).0044

$$K(s)=\begin{bmatrix} \dfrac{A-BB^T X-(1-\gamma^{-2})^{-1}ZYC^T C}{B^T X} & ZYC^T \\ -(1-\gamma^{-2})^{-1}C & 0 \end{bmatrix} \tag{9}$$

In the (8), $Z=(I-\gamma^{-2}YX)^{-1}$ and the X is the solution of RICCATI Equation in (9):

$$\begin{aligned} A^T X+XA-XBB^T+(1-\gamma^{-2})^{-1}C^T C=0 \\ AY+YA^T-YC^T CY=0 \end{aligned} \tag{10}$$

In the solving process, the most critical is to select the appropriate weighting functions. By choosing the appropriate weighting function, the control system can meet the design requirements. The sensitivity function S is the transfer function from disturbance input to output, and also can be regarded as the transfer function from system input to the tracking error. In the ideal case, the anti-interference ability of the system is stronger, and the output error of the system is smaller. So a small gain for the sensitivity function is wanted in the low-frequency of the system. The complement sensitivity function T is an index to measure the output of system affected by multiplicative disturbance, therefore, a large sheared frequency and a larger gain of system in the high frequency of the compensation sensitivity is required. So the weighted functions are selected as:

$$\left.\begin{aligned} W_1&=\frac{10s+2.5}{12s+50} \\ W_2&=\frac{0.01s^2+s+0.05}{10(s^2+s+s)} \\ W_3&=1 \end{aligned}\right\} \tag{11}$$

W_1 is chosen as low pass filter and reduce the gain in low frequency appropriately in order to satisfied dynamic characteristics; The system has a strong anti-interference ability, while reducing output error. W_2 is designed as a high pass filter to reduce the signal amplitude, to guarantee the robust stability of the system controller. W_3 is chosen as a constant usually. In order to achieve robust performance, the weighting functions need to satisfy the following inequality:

$$\left.\begin{aligned} \bar{\sigma}(S(j\omega))&\le\gamma\underline{\sigma}(W_1^{-1}(j\omega)) \\ \bar{\sigma}(R(j\omega))&\le\gamma\underline{\sigma}(W_2^{-1}(j\omega)) \\ \bar{\sigma}(T(j\omega))&\le\gamma\underline{\sigma}(W_3^{-1}(j\omega)) \end{aligned}\right\} \tag{12}$$

Using the LMI toolbox in MATLAB, the controller can get solved:

$$K(s)=\frac{-4213.6(s+3.864)(s+13.13)(s^2+s+1)(s^2+3.883s+35.07)}{(s+21.09)(s+5.005)(s+4.167)(s^2+1.019s+0.9572)(s^2+196.8s+13510)} \tag{13}$$

5. Controller Designed Based on M-Synthesis

In this section, the controller based on μ-synthesis is designed and solved via DK iteration.

5.1 Controller Designed Based on μ-Synthesis

In this part, a subarea of the ship integrated power system, shown in Fig.2, is chosen as the research object to explain the controller design process, due to the diesel generators and batteries have the same parameters, so the another subarea controller can be designed by the same method. So, the subarea LFC state space model can be extracted from (2):

$$\begin{aligned} \dot{x}&=A_1x+B_1u \\ y&=C_1x \end{aligned} \tag{14}$$

ISSN: 2414-1895 DOI: 10.6919/ICJE.201909_5(10).0044

Considering that the system parameters $T_{g1,2}$, $T_{d1,2}$, T_b, M and D are not invariant constants. However, it can be assumed that their values are changed within a certain intervals. Expressed as:

$$\left.\begin{aligned} T_{g1,2} &= \bar{T}_{g1,2}(1+p_{g1,2}\delta_{g1,2}) \\ T_{d1,2} &= \bar{T}_{d1,2}(1+p_{d1,2}\delta_{d1,2}) \\ T_b &= \bar{T}_b(1+p_b\delta_b) \\ M &= \bar{M}(1+p_M\delta_M) \\ D &= \bar{D}(1+p_D\delta_D) \end{aligned}\right\} \tag{15}$$

Where, $\bar{T}_{g1,2}$, $\bar{T}_{d1,2}$, $\bar{T}_b$, $\bar{M}$ and $\bar{D}$ are named as nominal values of $T_{g1,2}$, $T_{d1,2}$, T_b, M and D. The corresponding $p_{\square}$ and $\delta_{\square}$ in the expressions represent the possible perturbations on these seven parameters. In the present discuss, we let $p_{\square}=0.2$, and $\delta_{\square}\in[-1,1]$. This shown that the parameters uncertainties are perturbed in $\pm 20\%$. The subarea of LFC with uncertainty can be restructured as Fig.5.

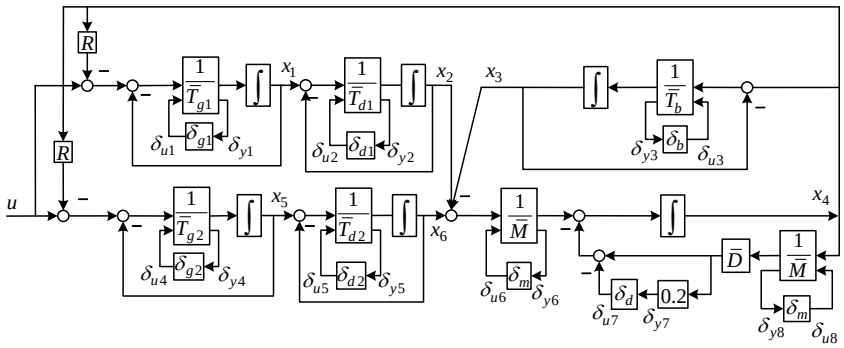

Fig.5 Load Frequency Control Subsystem with Uncertainty

The seven constant blocks in Fig.5 can be replaced by block diagrams in terms of $\bar{T}_{g1,2}$, $p_{g1,2}$ and $\delta_{g1,2}$ etc., in a unified approach. We note that the quantity $1/c$ may be represented as a lower LFT in δ_c

$$\begin{aligned} \frac{1}{c} &= \frac{1}{\bar{c}(1+0.2\delta_c)} = \frac{1}{\bar{c}} - \frac{0.2}{\bar{c}}\delta_c(1+0.2\delta_c)^{-1} \\ &= F_l(M_c,\delta_c) \end{aligned} \tag{16}$$

In the perturbation model, the parameters T_g, T_d, T_b and M can be transformed via lower LFT, and the different parameter D should be transformed via upper LFT expressed by:

$$D=\bar{D}(1+0.2\delta_d) = F_u(M_D,\delta_d) \tag{17}$$

Where $M_c=\begin{bmatrix} \frac{1}{\bar{c}} & -\frac{0.2}{\bar{c}} \\ 1 & -0.2 \end{bmatrix}$, $M_D=\begin{bmatrix} \bar{D} & -1 \\ 0 & 0.2\bar{D} \end{bmatrix}$.

With the above transformations and substitutions, the interconnection matrix is established, in the matrix, all of the system inputs, uncertainties input, and the system output, uncertainties output are contained.

$$\begin{bmatrix} \dot{x}_p \\ \delta_{yq} \\ y \end{bmatrix} = \begin{bmatrix} G_{11} & G_{12} & G_{13} \\ G_{21} & G_{22} & G_{23} \\ G_{31} & G_{32} & G_{33} \end{bmatrix} \begin{bmatrix} x_p \\ \delta_{uq} \\ u \end{bmatrix} \tag{18}$$

$$\delta_{uq}^T = diag[\delta_{g1},\delta_{d1},\delta_b,\delta_{g2},\delta_{d2},\delta_m,\delta_d,\delta_m]\cdot\delta_{yq}^T \tag{19}$$

In the equation, $p=1,2,...,6$, $q=1,2,...,8$. Both the elements in the input matrix $\left[\dot{x},\delta_{yq},y\right]^T$, output matrix $[x,\delta_{uq},u]^T$ and interconnection matrix $G_{ij}, ij=1,2,3$ and the uncertain block matrix have shown in Appendix.

In order to make a trade-off among different performance requirements, the weight functions should be designed, and according to the experience, the weight functions are chosen as following. The function $w_e(s)$ is selected to be large at low frequency in order to make a good regulation via weighted

ISSN: 2414-1895 DOI: 10.6919/ICJE.201909_5(10).0044

the control error. And the function $w_u(s)$ is designed to avoid the large overshoot and ensure the robustness via weighted the control input.

$$w_e(s) = \frac{10s+1}{20s} \tag{20}$$

$$w_u(s) = \frac{0.05s}{0.01s+1} \tag{21}$$

Take the parameters into the established interconnection matrix, and the μ-synthesis controller is solved by DK iterative algorithm. The μ-synthesis toolbox provided in MATLAB can conveniently deal with the μ-synthesis problem and the *dkit* command implement the DK iterative algorithm.

After the DK process, the iterations results show in Tab.2. From the table, both the value of μ and γ are large than 1 after the first iteration， which means that the robust stability(RS) and robust performance(RP) are not guaranteed. After the second iteration, the value of μ and γ are reduced less than 1, it is indicated the system robust stability and robust performance have reached. After the third iteration, the values are further reduced and the system robust stability and robust performance are further improved. As the iterations increase, the values of γ and μ continue to decrease, but the variation is small enough to disregard, and the index of robust stability and the index of robust performance are no longer changed. From the table, we also can see that the more iterations, the higher of the controller orders, in other words, too many iterations make the controller more conservative, what is unnecessary.

Tab. 2 DK iteration results

Iterations	K order	D order	γ value	μ value	μ-RS	μ-RP
1	6	0	8.777	1.498	1.172	1.351
2	8	2	0.744	0.520	0.202	0.506
3	12	6	0.439	0.436	0.202	0.506
4	20	14	0.390	0.389	0.202	0.506
5	20	14	0.369	0.369	0.202	0.506
6	30	24	0.360	0.359	0.202	0.506
7	30	24	0.353	0.352	0.202	0.506
8	32	26	0.349	0.349	0.202	0.506
9	32	26	0.348	0.348	0.202	0.506
10	34	28	0.347	0.347	0.202	0.506

By analysis, the robust stability index is 0.202, what indicated that the robust stability of the load frequency control system is achieved, *i.e.*, the system stability is guaranteed for $\|\Delta\|_\infty < 1/0.202$. And the robust performance index is 0.506, what indicated that the controller designed by μ-synthesis for the load frequency control system has achieved both the nominal performance and robust performance since:

$$\left\| \begin{bmatrix} W_p(I+F(G,\Delta)K)^{-1} \\ W_u K(I+F(G,\Delta)K)^{-1} \end{bmatrix} \right\|_\infty < 0.506 \tag{22}$$

for every diagonal Δ, $\|\Delta\|_\infty < 1$.

In order to get a compromise between the controller order and robust index, the result which iterated five times is adopted to design the controller. However, the order of controller is still much higher than the order of plant transfer function. It is means that, the implementation of the high-order controller in the ship integrated power system requires more hardware equipments and brings more

ISSN: 2414-1895 DOI: 10.6919/ICJE.201909_5(10).0044

maintenance problems, which greatly increases the cost of the controller and reduces the reliability of the controller. So, it is necessary to reduce the controller order to obtain a low order controller. And the HANKEL norm approximation method is adopted in the paper to implement the order reduction. After five iterations, the order of controller K_μ is 20, and reduced to 5 by HANKEL norm approximation. The controller transfer function is expressed as:

$$K_\mu = \frac{b_0 s^5 + b_1 s^4 + b_2 s^3 + b_3 s^2 + b_4 s^1 + b_5}{a_0 s^5 + a_1 s^4 + a_2 s^3 + a_3 s^2 + a_4 s^1 + a_5} \tag{23}$$

$b_i = [3.402 \times 10^{-8}, 10.26, 1.611 \times 10^4, 3.879 \times 10^5, 2.729 \times 10^6, 5.409 \times 10^6]$,

$a_i = [1, 1575, 5.053 \times 10^4, 4.256 \times 10^5, 1.251 \times 10^6, 1.422 \times 10^6]$.

6. Verification and Simulation

In this section, the controller designed by $H\infty$ and μ-synthesis for LFC on HIPS is verified and simulated.

Firstly, the transient responses of the two controllers are verified and the classical PID controller results are used as comparison. Fig.14 indicates the frequency deviation of AREA 1 and 2 when the system disturbed by 10% rated. When the AREA 1 receives the impulse, AREA 2 also will be disturbed via the tie-line. In Fig.14.a, the frequency variation of AREA 1 is suppressed in $\pm 0.01Hz$ by μ-synthesis. The controller performance based on μ-synthesis is obviously superior to the $H\infty$ optimal controller which suppressed the frequency variation in $\pm 0.04Hz$. Both of the two are much superior to the classical PID controller. It is also shows that the μ-synthesis converged the result in $2s$, the response is much faster than $H\infty$ controller. In Fig.14.b, the $H\infty$ optimal controller suppressed the AREA 2 frequency variation in $\pm 0.002Hz$, superior than μ-synthesis controller.

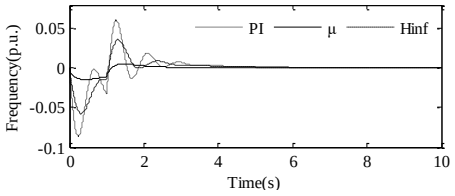

(a) Frequency Deviation in Area 1

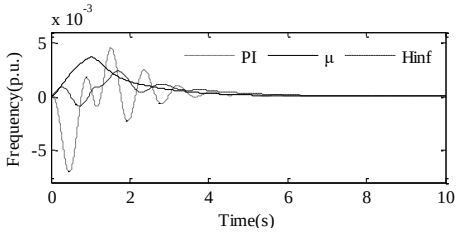

(b) Frequency Deviation in Area 2

Fig. 14 Frequency variation of step disturbance

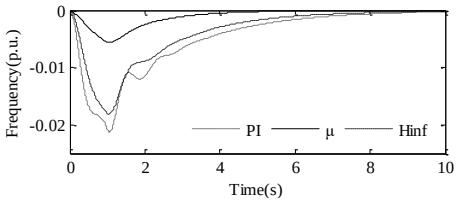

Fig.15 Tie line power of the step disturbance

The power on tie-line reflects the magnitude and direction of the exchange power between region 1 and region 2. The instantaneous output power is increased when the disturbance impacted AREA 1, and the power injected into the AREA 2 via tie-line. It can be seen from Fig.15 that the controller based on μ-synthesis keep the variation in $0.005Kw(p.u.)$, much smaller than the $H\infty$ controller.

ISSN: 2414-1895 DOI: 10.6919/ICJE.201909_5(10).0044

Secondly, the influence of parameter perturbation to the system is simulated. In Fig.16, it can be seen that in the worst case of parameter perturbation, the frequency deviation in AREA 1 is ranged in $\pm 0.01Hz$ by μ-synthesis, which is much smaller than the $H\infty$ controller. Because of the indirect influence of AREA 1 parameters perturbed on region 2, the frequency deviation of AREA 2 is smaller, however the μ controller still guarantees the system frequency has small fluctuation and relatively gentle change.

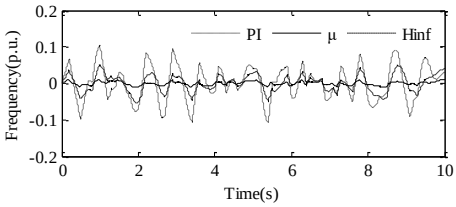

(a) Frequency Deviation in Area 1

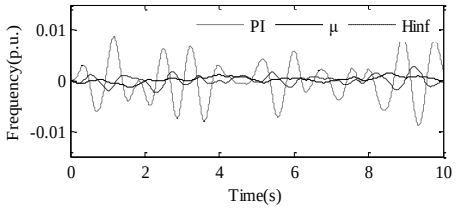

(b) Frequency Deviation in Area 2

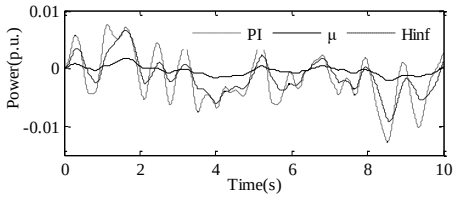

(c) Tie-line Power Deviation

Fig. 16 Output by parameter perturbation

7. Conclusion

In this paper, the robust approaches are used for load frequency control in ship integrated power system what is composed of diesel generators and batteries. The linear state space model of LFC problem is established. Considering the parameters perturbation, the uncertainty block is separated from the state space model. Then, the H∞ controller based on mixed sensitivity principle and μ-synthesis controller based on structure singular value are studied respectively and the robust stability and robust performance are verified in frequency domain. And the results are simulated under the computer environment and compared with classical PI controller. It is shown that both the H∞ and μ-synthesis controllers have good performance than PI controller and due to the μ-synthesis controller considering structured parametric uncertainties provides better performance than the H∞ control method.

Acknowledgments

This Project was supported by the National Natural Science Foundation of China (61573240) & Doctorial Innovation Foundation of Shanghai Maritime University (2016YCX067)

References

[1] Dupriez, R. F., L. Loron, and F. Claveau, "Design and optimization of an hybrid sailboat by a power modeling approach," *IEEE Electric Ship Technologies Symposium*, ESTS 2009, p 270-277(2009).

[2] Hongda L., Q. Zhang, and X. Qi, "Estimation of PV output power in moving and rocking hybrid energy marine ships," *Applied Energy*, Vol. 204, pp 362-372(2017).

ISSN: 2414-1895 DOI: 10.6919/ICJE.201909_5(10).0044

[3] Banaei M. R., and R. Alizadeh, "Simulation-Based Modeling and Power Management of All-Electric Ships Based on Renewable Energy Generation Using Model Predictive Control Strategy," *IEEE Intelligent Transportation Systems Magazine,* Vol. 8 No.2, pp. 90-103 (2016).

[4] Zahedi B, L. E. Norum, and K. B. Ludvigsen, "Optimized efficiency of all-electric ships by dc hybrid power systems", *Journal of Power Sources,* Vol. 255, pp. 341-354 (2014).

[5] Seenumani G., H. Peng, J. Sun, "A reference governor-based hierarchical control for failure mode power management of hybrid power systems for all-electric ships," *Journal of Power Sources,* Vol. 196, No. 3 pp. 1599-1607 (2011).

[6] Ovrum E., and T. F. Bergh, "Modeling lithium-ion battery hybrid ship crane operation," *Applied Energy,* Vol. 152, pp. 162-172(2015).

[7] Chen C, X. Wang, and J Xiao, "An energy allocation strategy for hybrid ship DC power system based on genetic algorithm," *Iete Journal of Research,* Vol. 62, No. 03, pp. 1-7(2015).

[8] Trovão J P, F. Machado, and P. G. Pereirinha, "Hybrid electric excursion ships power supply system based on a multiple energy storage system," Iet Electrical Systems in Transportation, Vol. 6, No. 3, pp. 190-201(2016).

[9] Zhu L, J. Han, and D. Peng, "Fuzzy logic based energy management strategy for a fuel cell/battery/ultra-capacitor hybrid ship," *2014 1st International Conference on Green Energy,* ICGE 2014, pp. 107-112(2014).

[10] Mathew J, P. P. Rajeevan, and K. Mathew, "A Multilevel Inverter Scheme With Dodecagonal Voltage Space Vectors Based on Flying Capacitor Topology for Induction Motor Drives," *IEEE Transactions on Power Electronics,* Vol. 28, No. 1, pp. 516-525(2013).

[11] Mohanty, B., S. Panda, and P. K. Hota, "Controller parameters tuning of differential evolution algorithm and its application to load frequency control of multi-source power system," International Journal of Electrical Power and Energy Systems, Vol. 54, pp. 77-85(2014).

[12] Kumari, S., G. Shankar, and S. Gupta, S, "Study of load frequency control by using differential evolution algorithm," *1st IEEE International Conference on Power Electronics,* Intelligent Control and Energy Systems, ICPEICES 2016, February 13, 2017.

[13] Mahto, Tarkeshwar and V. Mukherjee, "A novel scaling factor based fuzzy logic controller for frequency control of an isolated hybrid power system," *Energy,* Vol. 130, pp. 339-350(2017).

[14] Sahu, R. K., S. Panda, and N. K. Yegireddy, "A novel hybrid DEPS optimized fuzzy PI/PID controller for load frequency control of multi-area interconnected power systems," *Journal of Process Control,* Vol. 24, No. 10, pp. 1596-1608(2014).

[15] Sondhi S, and Y. V. Hote, "Fractional order PID controller for load frequency control," *Energy Conversion & Management,* Vol.85, No.9, pp. 343-353(2014).

[16] Pan I, and S.Das, "Fractional-order load-frequency control of interconnected power systems using chaotic multi-objective optimization," *Applied Soft Computing,* Vol. 29,pp. 328- 344(2015).

[17] Farahani M, S. Ganjefar, and M. Alizadeh, "PID controller adjustment using chaotic optimisation algorithm for multi-area load frequency control," *Iet Control Theory & Applications,* Vol. 6, No.13, pp. 1984-1992(2012).

[18] Liu X, H. Nong, and K. Xi, "Robust Distributed Model Predictive Load Frequency Control of Interconnected Power System," *Mathematical Problems in Engineering,* Vol. 2013, No. 4, pp. 1-10(2013).

[19] Mohamed T H, J. Morel, and H. Bevrani, "Model predictive based load frequency control design concerning wind turbines," *International Journal of Electrical Power & Energy Systems,* Vol. 43, No. 1, pp. 859-867(2012).

[20] Mohamed T H, H. Bevrani, A. A. Hassan, "Decentralized model predictive based load frequency control in an interconnected power system," *Energy Conversion & Management,* Vol. 52, No. 2, pp. 1208-1214(2011).

[21] Shiroei M, M. R. Toulabi, A. M. Ranjbar, "Robust multivariable predictive based load frequency control considering generation rate constraint," *International Journal of Electrical Power & Energy Systems,* Vol.46, No. 1, pp. 405-413(2013).

ISSN: 2414-1895 DOI: 10.6919/ICJE.201909_5(10).0044

[22] Ashouri-Zadeh, A., M. Toulabi, and A. M. Ranjbar, "Coordinated design of fuzzy-based speed controller and auxiliary controllers in a variable speed wind turbine to enhance frequency control," *IET Renewable Power Generation*, Vol. 10, No. 9, pp. 1298-1308(2016).

[23] Chaoxu, M., Y. Tang, and H. He, "Improved Sliding Mode Design for Load Frequency Control of Power System Integrated an Adaptive Learning Strategy," *IEEE Transactions on Industrial Electronics*, Vol. 64, No. 8, pp. 6742-6751(2017).

[24] Prasad, S., S. Purwar, and N. Kishor, "H-infinity based non-linear sliding mode controller for frequency regulation in interconnected power systems with constant and time-varying delays," *IET Generation, Transmission and Distribution*, Vol. 10, No. 11, pp. 2771-2784(2016)

[25] Prasad, S., S. Purwar, and N. Kishor, "Non-linear sliding mode load frequency control in multi-area power system," *Control Engineering Practice*, Vol. 61, pp. 81-92(2017).

[26] Chuang, N., "Robust H∞ load-frequency control in interconnected power systems," *IET Control Theory and Applications*, Vol. 10, No. 1, pp. 67-75(2016).

[27] Han, Y., P. M. Young, A. Jain, and D. Zimmerle, "Robust control for micro-grid frequency deviation reduction with attached storage system," *IEEE Transactions on Smart Grid*, Vol. 6, No. 2, pp. 557-565(2015).

Appendix

The matrices in expression (2) are:

$$A=\begin{bmatrix} -\frac{1}{T_{g1}} & 0 & 0 & -\frac{1}{R\cdot T_{g1}} & 0 & 0 & 0 & 0 & 0 \\ \frac{1}{T_{d1}} & -\frac{1}{T_{d1}} & 0 & 0 & 0 & 0 & 0 & 0 & 0 \\ 0 & 0 & -\frac{1}{T_{b1}} & \frac{1}{T_{b1}} & 0 & 0 & 0 & 0 & 0 \\ 0 & \frac{1}{M_1} & -\frac{1}{M_1} & -\frac{D_1}{M_1} & 0 & 0 & 0 & 0 & 0 \\ 0 & 0 & 0 & T_{12} & 0 & 0 & 0 & 0 & -T_{12} \\ 0 & 0 & 0 & 0 & 0 & -\frac{1}{T_{g2}} & 0 & 0 & -\frac{1}{R\cdot T_{g2}} \\ 0 & 0 & 0 & 0 & 0 & \frac{1}{T_{d2}} & -\frac{1}{T_{d2}} & 0 & 0 \\ 0 & 0 & 0 & 0 & 0 & 0 & 0 & -\frac{1}{T_{d2}} & -\frac{1}{T_{d2}} \\ 0 & 0 & 0 & 0 & 0 & 0 & \frac{1}{M_2} & -\frac{1}{M_2} & -\frac{D_2}{M_2} \end{bmatrix};$$

$$B=\begin{bmatrix} \frac{1}{T_{g1}} & 0 & 0 & 0 & 0 & \frac{1}{T_{g2}} & 0 & 0 & 0 \end{bmatrix}^T ; \quad C=\begin{bmatrix} 0 & 0 & 0 & 1 & 0 & 0 & 0 & 0 & 0 \\ 0 & 0 & 0 & 0 & 0 & 0 & 0 & 0 & 1 \end{bmatrix};$$

In expression (18):

$$G_{11}=\begin{bmatrix} -\frac{1}{\bar{T}_{g1}} & 0 & 0 & -\frac{R_1}{\bar{T}_{g1}} & 0 & 0 \\ \frac{1}{\bar{T}_{d1}} & -\frac{1}{\bar{T}_{d1}} & 0 & 0 & 0 & 0 \\ 0 & 0 & -\frac{1}{\bar{T}_{b1}} & \frac{1}{\bar{T}_{b1}} & 0 & 0 \\ 0 & \frac{1}{\bar{M}} & -\frac{1}{\bar{M}} & -\frac{\bar{D}}{\bar{M}} & 0 & \frac{1}{\bar{M}} \\ 0 & 0 & 0 & -\frac{R_2}{\bar{T}_{g2}} & -\frac{1}{\bar{T}_{g2}} & 0 \\ 0 & 0 & 0 & 0 & \frac{1}{\bar{T}_{d2}} & -\frac{1}{\bar{T}_{d2}} \end{bmatrix};$$

ISSN: 2414-1895 DOI: 10.6919/ICJE.201909_5(10).0044

$$G_{12}=\begin{bmatrix} -\frac{0.2}{\bar{\bar{T}}_{g1}} & 0 & 0 & 0 & 0 & 0 & 0 & 0 \\ 0 & -\frac{0.2}{\bar{\bar{T}}_{d1}} & 0 & 0 & 0 & 0 & 0 & 0 \\ 0 & 0 & \frac{0.2}{\bar{\bar{T}}_{b1}} & 0 & 0 & 0 & 0 & 0 \\ 0 & 0 & 0 & 0 & 0 & -\frac{0.2}{\bar{\bar{M}}} & -1 & 0.2\frac{\bar{D}}{\bar{\bar{M}}} \\ 0 & 0 & 0 & -\frac{0.2}{\bar{\bar{T}}_{g2}} & 0 & 0 & 0 & 0 \\ 0 & 0 & 0 & 0 & -\frac{0.2}{\bar{\bar{T}}_{d2}} & 0 & 0 & 0 \end{bmatrix}; G_{13}=\begin{bmatrix} \frac{1}{\bar{\bar{T}}_{g1}} \\ 0 \\ 0 \\ 0 \\ \frac{1}{\bar{\bar{T}}_{g2}} \\ 0 \end{bmatrix};$$

$$G_{21}=\begin{bmatrix} -1 & 0 & 0 & -R_1 & 0 & 0 \\ 1 & -1 & 0 & 0 & 0 & 0 \\ 0 & 0 & -1 & 1 & 0 & 0 \\ 0 & 0 & 0 & -R_2 & -1 & 0 \\ 0 & 0 & 0 & 0 & 1 & -1 \\ 0 & 1 & 1 & 0 & 0 & -1 \\ 0 & 0 & 0 & 0.2\frac{\bar{D}}{\bar{\bar{M}}} & 0 & 0 \\ 0 & 0 & 0 & 1 & 0 & 0 \end{bmatrix}; G_{22}=\begin{bmatrix} -0.2 & & & & & & & \\ & -0.2 & & & & & & \\ & & -0.2 & & & & & \\ & & & -0.2 & & & & \\ & & & & -0.2 & & & \\ & & & & & -0.2 & & \\ & & & & & & -0.04\frac{\bar{D}}{\bar{\bar{M}}} & \\ & & & & & & & -0.2 \end{bmatrix}; G_{23}=\begin{bmatrix} 1 \\ 0 \\ 0 \\ 1 \\ 0 \\ 0 \\ 0 \\ 0 \end{bmatrix};$$

$$G_{31}=\begin{bmatrix} 0 & 0 & 0 & 1 & 0 & 0 \end{bmatrix}; G_{32}=zeros(1\times 8); G_{33}=0;$$